Sirte University Scientific Journal Vol. 13, No. 2 (2023) 1-12

Sirte University Scientific Journal (SUSJ)

Journal home page: http://journal.su.edu.ly/index.php/SUSJ/index

DOI: 10.37375/susj.v13i2.2498

Design and Simulation of Torque Gauge Using Piezo-Resistive Duplex Strain

M. Hilal Muftah[1], K. Petroczki[2], Omar M. Salih[3], A. A. Borhana[4] and E. Awad Khidir[5]

[1]*Department of Computer Science, Faculty of Information Technology, Sirte University, 674 Sirte, LIBYA.*
[2]*Department of Agra-energetics and Foods Engineering, Faculty of Mechanical Engineering, Szent Istvan University, H 2103, Godollo, HUNGARY).*
[1]*Department of Computer Science, Faculty of Information Technology, Sirte University, 674 Sirte, LIBYA.*
[4]*Department of Mechanical Engineering, College of Engineering, Universiti Tenaga Nasional, Putrajaya Campus, Jalan IKRAM-UNITEN, 43000 Kajang, Selangor, MALAYSIA.*
[5]*Department of Mechanical and Material Engineering, Faculty of Engineering and the Built Environment, Universiti Kebangsaan Malaysia, 43600 UKM Bangi, MALAYSIA.*

DOI: 10.37375/susj.v13i2.2498

ARTICLE INFO:
Received 23 August 2023.
Accepted 24 November 2023.
Available online 01 December 2023.

***Keywords**: Keywords:* duplex, modeling, rotating shaft, simulation, strain gauge,

A B S T R A C T

Practices of information technology in the field of engineering, especially in the field of designs in the science of mechanical engineering, have become an important matter in the technical world today. In this research, a torque measuring device has been designed and simulated using a Piezo resistive Duplex Strain as an alternative to a Piezoresistive V-shaped strain. The experimental factors in these fields are often associated with the precise measurement of strains found in the elastic region. Based on the software of ANSYS simulation result, a design of a piezo-resistive metal gauge on the solid shaft is created. Thus, a design incorporating the Piezo-Resistive Duplex Strain Gauge on the shaft of a torque sensor is performed. The results of the simulation revealed the amount of strain transferred from the shaft to the substrate, as well as to the gauge that can be attributed to the torque applied. Theoretical studies on the piezo-resistive metallic gauge found on a solid shaft as well as on the torque sensor are discussed. The maximum of 95.862με for every single Duplex Strain, as well as a maximum resistance change in gauge (grid) = 0.04Ω, is obtained for an applied torque value of 22.1Nm relating to the earlier design, which has a maximum of 127.29 με for using four sections and a maximum resistance change in gauge equal to 0.091Ω were achieved for an applied torque of 22.0725 Nm. It can be said that Modeling and Simulation have become an integral part of research and development across many fields of study, having evolved from a tool to a discipline in less than two decades. Modeling and Simulation Fundamentals offers a comprehensive and authoritative treatment of the subject matter and includes definitions, paradigms, and applications to provide skills needed to work successfully as developers and users of modeling and simulation.

***Corresponding author*: E-mail: muftah07@yahoo.com (An active e-mail address of the corresponding author)**

1 Introduction

A strain gauge transforms pressure, force, torque, weight, and tension into an observable and measurable alteration in electrical resistance. The principle of metal gauge operation is grounded on the belief that any electrical conductor can change its resistance when mechanical stress is applied (Yang et al. 2008). This is attributable to the variations in the cross-section of the conductor, as well as the resistivity caused by micro-structural changes. The strain gauge size is typically determined by the available space or the strain field topography. No physical constraint is present when selecting the gauge dimension (Joyce & Scott 1993). The equations of the strain gauge are obtained based on the small theory of deflection (Eaton et al. 1999; Szilard 1974). ANSYS, a known finite element tool, is used to identify the maximum strain distribution on the shaft. This enables the selection of the preferred orientation of the gauge and the appropriate active region to reach maximum sensitivity. The materials used as substrates for gauge design include polyimide, silicon, and aluminum (Hamid et al. 2006; Thingamajig et al. 2008; Yang&Lu 2013). Aluminum is the material used to generate the maximum strain in this study and is thus selected as the substrate for gauge design. Given its suitability for use at a good temperature range from -195˚C to +400˚C, as well as its ease of handling, aluminum is considered an ideal substrate for general dynamic and static stress analysis. Isoelastic alloy is used as the material for the gauge (grid) needed for the strain gauge design. This alloy is aluminum one of the most often-used piezo-resistive metal gauge materials. In addition, its high peel strength results in the fabrication of a gauge that is less sensitive to mechanical damage and wear during installation (Schomburg et al. 2004; Window&Holister 1982). As far as the authors are concerned, no theoretical study with a focus on the piezo-resistive metallic gauge on the solid shaft for the measurement of strain currently exists. Equations in this work are based on a piezo-resistive metallic gauge on the solid shaft for strain measurement. A torque sensor is fabricated using this strain gauge, and its corresponding individual components and strain distribution are evaluated. Moreover, a calculation is performed based on the percentage of strain transformed from one component to another. This feature could be used for the effective selection of the correct material for the design. Several disks for torque-measuring sensors technologically advanced into spoke-type assemblies, as an alternative, depiction strain on the right angles or cross spoke-surface with a twisting distortion approach (Wang Y.J. et al, 2017; Hu G.Y et al, 2018; Li X. et al, 2019). A Lever-Type Method of Strain Exposure for Disk F-Shaped Torque Sensor Design reported by (Ran Shu et al., 2020). This paper presents a lever-type method of strain exposure that performs a uniaxial tension and compression deformation mode to optimize strain uniformity and improve the trade-off. Moreover, based on this approach, the proposed disk F-shaped torque sensor enjoys axial thinness, easy installation of strain gauges, and flexible customization. The simulation and experimental results have validated the basic design idea. In the current studies, the scientists focus on the calibration of the strain gauges. For example, the development of a novel dynamic torque generation machine based on the principle of a Kibble balance (Misaki Hamaji et al, 2022). Calibration of a torque measuring device using an electromagnetic force torque standard machine (Atsuhiro Nishino and Kenichi Fujii, 2019). In Situ Calibration of Six-Axis Force–Torque Sensors for Industrial Robots with Tilting Base (Cheng Ding et al, 2022).

A simulation is the execution of a model, represented by a computer program that gives information about the system being investigated. In this paper, strain gauge measurements involve two expert fields, namely electrical engineering and mechanical engineering. In several resource checks, it is especially crucial to understand the stress, which frequently comes about in the materials. The idea will lead to a significant conclusion concerning the structural balance of a material, regardless of its preceding shape and size. The objectives of this paper were achieved through practical experience with resistance strain measurement procedures and an understanding of the actual Wheatstone connection, as well as just how it is utilized in strain measurements. The research was conducted into the layout as well as the simulation of piezoresistive material, as well as the torque sensor. The material that was purchased came with equations for determining the torsional base of the torque sensor. Aluminium was selected as an alternative substrate material for determining the desired strain. The most stretched places in the substrate were determined by different border problems. The determined pattern was designed as well as analyzed. The most stretched area and its equivalent pattern were picked for the determination of the strain. A torque sensor was designed using the actual design of the piezoresistive material with its determined strain, and the simulation results indicated that the resistance change was usually linear towards the utilized torque. The results of the simulation enabled the percentage of strain transported in the base from the shaft to the substrate and then to the gauge to be calculated. The actual purpose of this was to calculate the precise strain percentages of the sensor parts. In the end, the simulation approach of analyzing a model is opposed to the analytical approach, where the method of analyzing the system is purely theoretical. As this approach is more reliable, the simulation approach gives more flexibility and convenience (Muftah. et al, 2021).

In this design, a novel strain gauge was simulated for the preferred torque measurements as shown in Figure 1.

The space for the determined strained area, i.e., the active area for the gauge plan, was set at 3.76 mm x 2.678 mm, as shown in Figure 5. Moreover, a substrate with a length of 20 mm, width of 9 mm, and thickness of 0.5 mm was preferred in this study for the project and examination (Muftah. et al, 2021).

In this paper, the exact perseverance connected with the strain of components is very important for structural designs, analyses, and excellent control. The information linked to this type of test is usually related to the exact dimensions connected with the pressure within a flexible region. This paper proposed the design and simulation of a torque sensor with a piezoresistive V-shaped strain gauge. The piezoresistive measure of precious metal for a stable base was made according to the results of an ANSYS simulation. A torque sensor with a piezoresistive V-shaped tension measure on a base was made. The result of the particular simulation shifted the fraction of tension on the base to enable the torque on the substrate to be measured. Theoretical studies on the piezoresistive measure of metal for the stable base as well as the torque sensor were introduced. A maximum of 127.29 με and a maximum resistance change in gauge equal to 0.091Ω were achieved for an applied torque of 22.0725 Nm. Here, computer systems modeling and simulation are going to be used. Proper knowledge of both the techniques of simulation modeling and the simulated systems themselves is needed to achieve the new design (Muftah. et al, 2021).

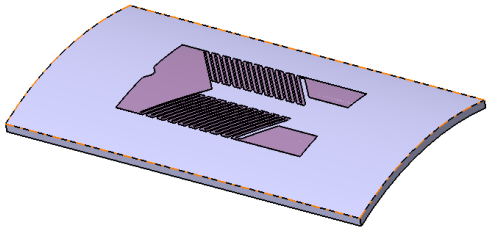

Fig. 1 Configuration of torsional strain gauge model

1.1 Material for the strain gauge

The Piezo resistive–Isoelastic material is selected for the strain gauge design in this study because of its high sensitivity, as shown in Table 1. Piezor resistive–Isoelastic material has been used commercially for other strain gauges, given that it possesses high fatigue strength (Yang&Lu 2013). For this reason, the strain gauge can normally be used in case the harmonic load has a strain value not greater than 1500με. However, the Wheatstone Bridge is used owing to its sensitivity to temperature.

Table 1 The sensitivity of several materials (Intiang et al. 2009)

Material	Sensitivity (K)
Platinum (Pt 100%)	6.1
Platinum-Iridium (Pt 95%, Ir 5%)	5.1
Platinum-Tungsten (Pt 92%, W 8%)	4.0
Isoelastic (Fe 55.5%, Ni 36% Cr 8%, Mn 0.5%) *	3.6
Constantan / Advance / Copel (Ni 45%, Cu 55%) *	2.1
Nichrome V (Ni 80%, Cr 20%) *	2.1
Karma (Ni 74%, Cr 20%, Al 3%, Fe 3%) *	2.0
Armour D (Fe 70%, Cr 20%, Al 10%) *	2.0
Monel (Ni 67%, Cu 33%) *	1.9
Manganin (Cu 84%, Mn 12%, Ni 4%) *	0.47
Nickel (Ni 100%)	-12.1

* Isoelastic, Constantan, Advance, Copel, Nichrome V, Karma, Armour D, Monel, and Manganin are all trade names owned by the respective owners.

1.2 Substrate Material

It is a known fact that there are several materials available for use as substrates without any effect on operations. Aluminium is selected as the substrate material of the strain gauge in this study because it is a very common material of choice. It is also inexpensive and very easy to attach with the use of cyanoacrylate or epoxy (Yang&Lu 2013). In Situ Calibration of Six-Axis Force–Torque Sensors for Industrial Robots with Tilting Base (Cheng Ding et al, 2022).

Using a special glue, strain gauges are fastened to the substrate. The selection of glue will rely on the required lifespan of the measurement system. For short-term requirements that cover several weeks, cyanoacrylate glue is preferred. However, epoxy glue is required for long-term use (Yang&Lu 2013).

Preparation of the surface includes smoothening (e.g. with very fine sandpaper), deoiling with solvents, and removing solvent traces. The strain gauge must then be fastened immediately to prevent the pollution of the prepared area and to avoid oxidation. If this procedure is not properly followed, surface binding may be unreliable and erroneous, and unpredictable measurement errors can occur. Strain gauge-based technology is generally utilized in the process of producing pressure sensors. The gauges in pressure sensors are generally made from polysilicon, metal film, bonded foil, or thick film (Yang&Lu 2013).

2 Theoretical Study

The change in gauge resistance on the shaft that results from an applied torque is determined by the strain generated on the shaft and delivered to the gauge. The process is discussed in detail in the succeeding subsections.

2.1 Strain on the Solid Shaft

The effective torsion moment M_t from which the transferred power P can be determined for a rotating shaft is identified (Korzenszky 2009; Muftah&Haris 2010). Thereafter, the full bridge strain can be computed based on equation (1):

$$\varepsilon_i = \frac{2\,M_t}{G \cdot S_p} \qquad (1)$$

Shear modulus *G* makes shear stress calculations less complex because there is no need to determine an independent material parameter, such as Young's modulus *E* and Poisson's ratio *ν*, but is rather based on the following (Hilal Muftah&Haris 2011; Hoffmann 1989; Young&Budynas 2002):

$$G = \frac{E}{2} * \frac{1}{1+\nu} = \frac{E}{2(1+\nu)}\ 0.385E\ for\ \nu\ 0.3 \qquad (2)$$

The following applies in the case of a cylindrical shaft:

$$S_p = \frac{\pi \cdot d^3}{16} \approx 0.2d^3 \qquad (3)$$

As a result, the greatest strain in the shaft was considered through the use of 127.29 με (1.2729E-04), for a full bridge circuit (4SGs) at torque, M_t = 22.0725Nm as shown in table 2. The bridge factor then was equal to 4, and the strain for each resistance was equal to 31.82με (3.181E-05).

Table 2 Strain in the Shaft

Case	Mass (Kg)	Force (N)	Torque (Nm)	Strain in Shaft (mm/mm)
1	0.00	0.0000	0.0000	0.0000
2	0.50	4.9050	2.4525	1.4143E-05
3	1.00	9.8100	4.9050	2.8286E-05
4	1.50	14.7150	7.3575	4.2430E-05
5	2.00	19.6200	9.8100	5.6573E-05
6	2.50	24.5250	12.2625	7.0716E-05
7	3.00	29.4300	14.7150	8.4859E-05
8	3.50	34.3350	17.1675	9.9002E-05
9	4.00	39.2400	19.6200	1.1315E-04
10	4.50	44.1450	22.0725	1.2729E-04

2.2 Strain on the Gauge

A strain gauge is a sensor that measures strain through electrical resistance changes. Once a material is strained, an increase in metallic material resistance is observed (Micro-Measurements 2007; Murray&Miller 1992). Whereas L is the length of the material, A is the area, and ρ is the Specific resistance then the Resistance (R) of the gauge is given by:

$$R=\rho\ L/A \qquad (4)$$

The interpretation reveals the relationship between the levels of resistor resistance and length, and the difference in resistance reveals the length variation. Strain is measured based on the change in the tolerable mechanical variation of the electrical signal with the use of a strain gauge. A strain gauge null point variation agreeing to the variation in temperature is known as a measuring error. Wheatstone bridge is typically used because of its advantage in enhancing the signal and calibrating temperature variation results. Thus, it makes additional precision measurement possible (Eberlein 2008; Zorob 2010). The Wheatstone bridge design utilizes four resistors, as shown in Figure 1. Three types of Wheatstone bridge constructions are available, namely Full Bridge, Half Bridge, and, when a single resistance is recycled in the Wheatstone bridge, a circuit construction called Quarter Bridge (Micro-Measurements 2007).
Then the voltage drop values of both resistances R1 and R4 with the use of the following equations and diagram can be determined:

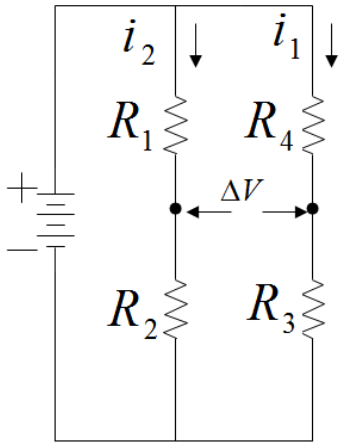

Fig. 2 Application of the Wheatstone Bridge circuit (Zeinali et al. 2014)

When torque is applied to the shaft (Zeinali et al. 2014), the resistance of strain gauges will change as below:

$$R_1 = R_3 = R_G + \Delta R$$
$$R_2 = R_4 = R_G - \Delta R \qquad (1)$$

R_G is strain gauge resistance before applying torque?

Equations of current and voltage:

$$V_{in} = i_1(R_1 + R_2) \Rightarrow i_1 = \frac{V_{in}}{R_1 + R_2}$$
$$V_{in} = i_2(R_3 + R_4) \Rightarrow i_2 = \frac{V_{in}}{R_3 + R_4} \qquad (2)$$

Figure 2, ΔV is:

$$\Delta V = i_1 R_1 - i_2 R_4 \qquad (3)$$

By substitution of equations (2) into (3):

$$\Delta V = V_{in}\left(\frac{R_1}{R_1 + R_2} - \frac{R_4}{R_3 + R_4}\right) \qquad (4)$$

Through the use of:

$$\Delta R / R_G = G.F \times \varepsilon \qquad (5)$$

So:

$$\Delta V = V_{in}(G.F \times \varepsilon) \qquad (6)$$

$$\Rightarrow \varepsilon = \frac{\Delta V}{G.F \times V_{in}} \qquad (7)$$

The changes in strain gauge resistance are derived by using Equation (5), whereas the changes in gauge voltages are determined using Equation (7) for the measurements on a shaft under the torsion (Full Bridge) case (Zeinali et al. 2014). Measurements on a shaft under rotation (Full Bridge) that has temperature compensation reveal that strain gauges 1 and 3 are positive, whereas strain gauges 2 and 4 are negative (Eberlein 2008). However, when standard and bending strains are compensated, strain gauges 1 and 4 are positive, whereas strain gauges 2 and 3 are negative (Eberlein 2008). Every stage under the Wheatstone Bridge Circuit uses a total of four resistors, each of which can consist of only one, two, or four strain gauges. The maximum output value can be derived if four active strain gauges are used. Moreover, modern amplifiers complete the "missing" resistors in the Wheatstone Bridge Circuit (Eberlein 2008; Micro-Measurements 2007).

2.3 Variations in Temperature

A large number of effects may come from temperature variations. The object size will change because of thermal expansion, which can be detected as strain by the gauge. There can be changes in the resistance of the

gauge, as well as of the connecting wires. In general, most strain gauges are made using a constantan alloy (Yang&Lu 2013). Numerous Karma and constantan alloys have been employed to enable the effects of temperature on strain gauge resistance to nullify the change in gauge resistance caused by the thermal expansion of the object under test. Given that different materials have different levels of thermal expansion, self-temperature compensation (STC) requires the selection of a specific alloy that is suitable for the material of the object under test. Strain gauges that are not self-temperature-compensated (such as Isoelastic alloy) can be temperature-compensated by using the dummy gauge technique, where a dummy gauge (identical to the active strain gauge) is installed on an unstrained sample having the same material as the test specimen. The sample with a dummy gauge is placed in thermal contact with the test specimen near the active gauge. The dummy gauge is then wired into a Wheatstone bridge on an arm that is adjacent to the active gauge so that the effects of temperature on both the dummy and active gauges nullify each other (Yang&Lu 2013).

3 Torque Measurement

After the biaxial a couple of elements also referred to as torsion, as well as the fishbone strain gauge, can be cemented using an example of the beauty that's beneath torsion, in a way that its central axis coincided with the axis connected with torsion and the grid-lines connected with its just one factor are near ±45° to the axis, this connection result can be hypersensitive on the torque but insensitive to help virtually any axial loads as well as bending (Muftah et al. 2013; Prombonas et al. 2013).
Device dynamic error is one of the faults that is challenging to estimate. In the context of research on the energy of agricultural equipment, the process for creating this inaccuracy in the example of torsional torque dynamometers is short-regarded as the most prevalent. The limiting ratios of the external impacts' frequencies and the natural vibrations of strain-measuring equipment are provided. In torque strain analysis, recommendations are provided to lower dynamic error. The recommendations for decreasing dynamic errors in torque measurements are made possible by the current review and the cumulative experience of strain gauge research. A strain gauge needs to have the least amount of torque inertia to maintain its inertial characteristics in response to changes in torque (Yu P Manshin et al, 2021).

Based on the results of the ANSYS simulation, the piezo-resistive V-shaped strain gauge is used to guide the torque sensor design. In the torque sensor design, the strain gauge is fixed, and a Wheatstone circuit with a duplex strain gauge, as shown in Figure 2, is developed to measure the strain on the shaft when the load is applied to the end of the shaft. The figure below shows the method for torque measurement using strain gauges. The torque is measured by the strain sensor fastened to the shaft with a diameter (d) = 28 mm. In this case, a total of four active bridges are attached to the sensor, as shown in Figure 3.

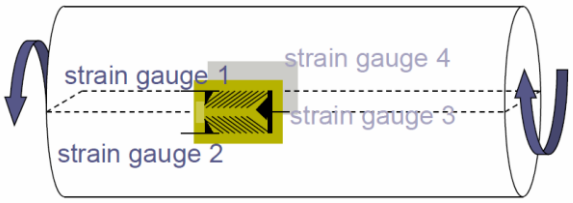

Fig. 3'd' twisted shaft diameter and torsion strain gauge (Eberlein 2008)

4 Simulation

To identify the strain distribution and perform the strain calculation on the sensor components, the finite element analysis software ANSYS is used (Cao et al. 2000; Lin et al. 1999; Orhan et al. 2001). CATIA software is a tool used for the design of sensor components, such as substrate, shaft, and strain gauge. The strain gauge and torsional shaft part dimensions are only considered for geometric analysis. These dimensions are employed to modify all equipment in CATIA software for export to a STEP file. In addition, the STP file generated by CATIA software and the mesh of the model is imported for simulation. Then, the data is transferred to the Steady-State module of WORKBENCH for further simulation.

To locate the maximum strained area on the shaft, the strain distribution is used, as shown in Figure 3. This configuration enables the fabrication of highly sensitive strain gauges. However, sensor component strain calculation is used to identify the percentage of strain transferred from one component to another. This helps in identifying the maximum strained components, the values of which are given in Tables 3 and 6.

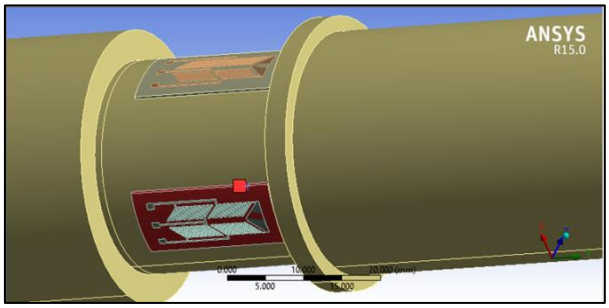

Fig. 4 Location of the duplex strain gauges and load based on boundary conditions

5 Strain Gauge

This study simulates an innovative strain gauge for analysis and design based on torque measurements. The area covered by the maximum strained region, the active region for gauge design, is found to be 3.76 mm × 2.55 mm, as shown in Figure 5. In addition, a substrate with a length of 20 mm, width of 9 mm, and thickness of 0.5 mm is selected in this study for the analysis and design.

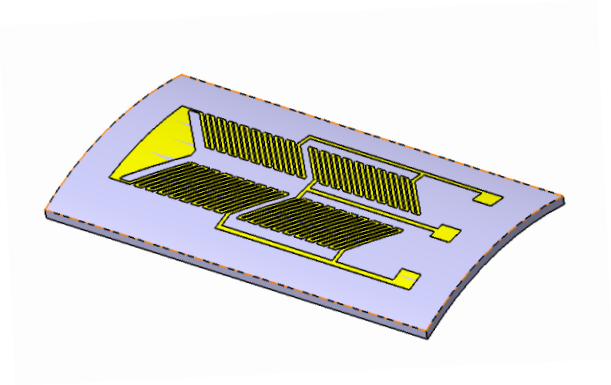

Fig. 5 Configuration of the new duplex strain-gauge model

The substrate simulation was conducted under the clamped and supported edge boundary conditions. As shown in Figure 5, the minimum and maximum strained locations of the clamped and supported edge substrates are labeled. In this figure, the maximum strain locations for supported edges are at the long side edges. Given that the minimum strained locations are at the canter, the gauge design in this area is considered insensitive. Thus, the clamped edge boundary condition is employed for the strain gauge design. The substrate mesh element matrix size is 200 × 90 divisions based on its dimensions of 20 mm × 9 mm. The mesh element matrix size should not exceed 200 × 90 because of the convergence limitation. An increase in matrix division increases the strain. However, the maximum strain distribution area is shifted towards the long side edges. The maximum strain distribution area remains at the canter, but its strain value is reduced for smaller matrix dimensions. Thus, the maximum strain value and its corresponding strain area are cantered on convergence limitations.

In this study, an eight-loop strain gauge is designed to be consistent with the ones used in the industry. A gauge (grid) pattern with active length = 2.55 mm, single line width values = 0.4 mm and 0.07 mm, and thickness = 0.005 mm is designed and assembled on the identified maximum strained area. The shaft and gauge are independently meshed while sustaining continuity, as shown in Figure 6. Given that the maximum strain (shown in black) is located at the canter area and that the area near the shaft diameter is 28 mm, the piezo-resistive gauge should be placed within this location.

Shown in Figure 6 is the strain variation, including matrix divisions. The value of matrix division increases, shifting to the maximum strained location towards the long side edges. Figure 7 is the representation of the maximum strain developed. The creation of geometry and meshing is necessary before the use of ANSYS meshing to simulate the problem. The geometry aspect can be addressed using CAD software, such as CATIA, ANSYS GEOMETRY, and SOLIDWORKS. Meanwhile, meshing can be performed using ICEM CFD, ANSYS meshing, and HYPERMESH. Meshing is an essential step in FEA because it influences the convergence process. For the most accurate results, a fine mesh is required for piezo-resistive modeling. In addition, the mesh shaped using the ANSYS meshing tool is used to manage the mesh size. The mesh and time steps are inherent components of the model. The strain gauge models utilize the grid scale. In cases where the mesh is too anisotropic to resolve, a longer length scale may hurt the results. Thus, the use of isotropic grids, as well as the use of tetrahedral in place of hexahedral elements, may be considered.

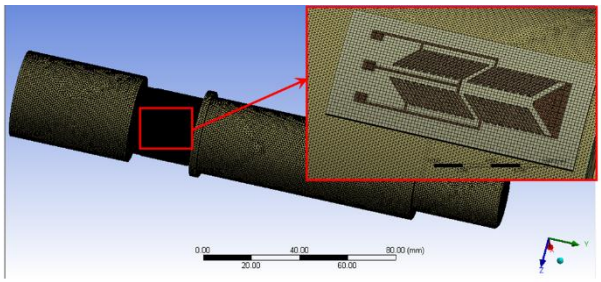

Fig. 6 Elements and meshing shape of duplex strain gauge

The gauge (grid) pattern design on the red region enables the achievement of maximum sensitivity. The gauge pattern is also meant to serve as a basis for the design and analysis of the duplex strain gauge. The linear variation of length alteration concerning the applied torque on the strain gauge is shown in Figure 7. The results are shown in Tables 3 to 6. In addition, the strains on the substrate and gauge are independently calculated, and Table 4 determines the maximum strained area on the substrates.

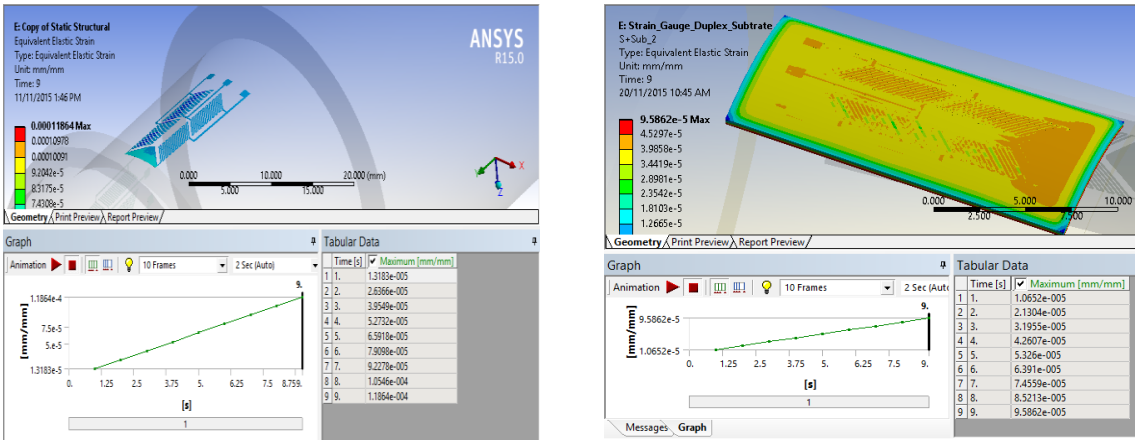

Fig. 7 Design and analysis of the form of duplex strain gauge

Table 1 Strain in the duplex strain gauge

Case	Mass (Kg)	Force (N)	Torque (Nm)	Simulation duplex strain-gauge (mm/mm)
1	0.00	0.0000	0.0000	0.0000
2	0.50	4.9050	2.4525	1.3183E-05
3	1.00	9.8100	4.905	2.6366E-05
4	1.50	14.7150	7.3575	3.9549E-05
5	2.00	19.6200	9.81	5.2732E-05
6	2.50	24.5250	12.2625	6.5918E-05
7	3.00	29.4300	14.715	7.9098E-05
8	3.50	34.3350	17.1675	9.2278E-05
9	4.00	39.2400	19.62	1.0546E-04
10	4.50	44.1450	22.0725	1.1864E-04

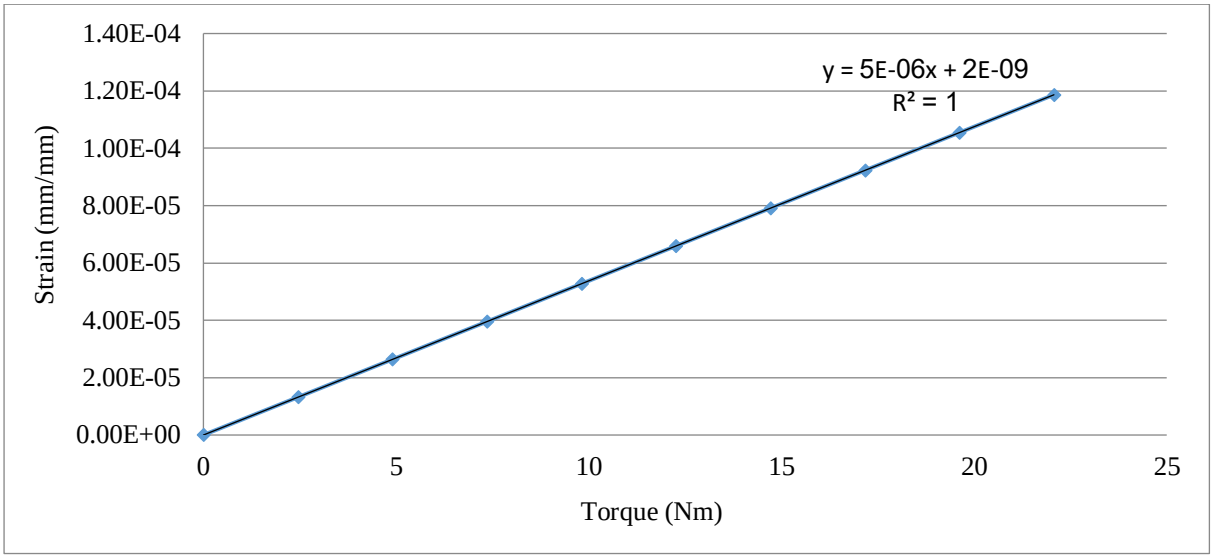

Fig. 8 The strains on the duplex gauge when torque is applied

Table 2 Strain in Substrates

Case	Mass (Kg)	Force (N)	Torque (Nm)	Strain in substrate (mm/mm)
1	0.00	0.0000	0.0000	0.0000
2	0.50	4.9050	2.4525	1.0652E-05
3	1.00	9.8100	4.905	2.1304E-05
4	1.50	14.7150	7.3575	3.1955E-05
5	2.00	19.6200	9.81	4.2607E-05
6	2.50	24.5250	12.2625	5.3260E-05
7	3.00	29.4300	14.715	6.3910E-05
8	3.50	34.3350	17.1675	7.4559E-05
9	4.00	39.2400	19.62	8.5213E-05
10	4.50	44.1450	22.0725	9.5862E-05

In terms of the torque applied to the strain gauge, the linear variation of strain change is shown in Figure 7. This result reveals that gauge resistance has a linear response to the applied torque. The maximum applied torque and its corresponding strain obtained for the aluminum substrate are 22.0725 Nm and 95.862 με, respectively. The substrate material showed a non-linear reaction when the applied torque was larger than the aforementioned values. These results were obtained through ANSYS simulation.

6 Torque Sensor

A torque sensor is designed and evaluated with the respective use of ANSYS and CATIA software. The torque sensor components include a solid shaft, substrate, and gauge. In this study, a 28 mm diameter shaft with the maximum strain distribution is selected. Meanwhile, the minimum strains are generated on the large diameter of the shaft. Thus, the strain gauge is fixed at the maximum strain area to achieve maximum sensitivity. Figure 6 reveals the strain distribution on such sensor components as the shaft, substrate, and gauge. The strain formed on the torque sensor and its components are listed in Tables 3 and 4. Such information can be used to compute the percentage of strain transformation from one component to another, such as the shaft, substrate, or gauge (grid). These results also facilitate the observation of material performance under different loads. In addition, this analysis enables the selection of the appropriate material, orientation, and dimension of components before fabrication.

Accordingly, the percentages of the transformed strain from the shaft to the substrate and then to the gauge are calculated and provided in Table 5, respectively. The amount of transformed strain from the substrate to the grid is constant for all torque levels, which suggests that the gauge (grid) pattern is designed exactly on the maximum strained location of the substrate, thereby enabling the achievement of the maximum sensitivity

Table 3 Torque sensor results

Case	Torque (Nm)	Simulation duplex strain-gauge (mm/mm)	Strain in substrate (mm/mm)	Strain in Shaft (mm/mm)	Strain transferred from substrate to gauge	Strain transferred from the shaft to the substrate
1	0	0	0	0	0	0
2	2.4525	1.3183E-05	1.0652E-05	1.4143E-05	123.76080	75.31539
3	4.905	2.6366E-05	2.1304E-05	2.8286E-05	123.76080	75.31539
4	7.3575	3.9549E-05	3.1955E-05	4.2430E-05	123.76467	75.31304
5	9.81	5.2732E-05	4.2607E-05	5.6573E-05	123.76370	75.31363
6	12.2625	6.5918E-05	5.3260E-05	7.0716E-05	123.76643	75.31539
7	14.715	7.9098E-05	6.3910E-05	8.4859E-05	123.76467	75.31304
8	17.1675	9.2278E-05	7.4559E-05	9.9002E-05	123.76507	75.31034
9	19.62	1.0546E-04	8.5213E-05	1.1315E-04	123.76046	75.31274
10	22.0725	1.1864E-04	9.5862E-05	1.2729E-04	123.76124	75.31068

In the tables above, it was noted that the output results for the four strain gauges were almost four times the output values of the one strain gauge. What is more, in the case of the two strain gauges, the values were approximately twice the output values of the one strain gauge that was recycled in this research. The values of the resistance changes of the four strain gauges of 350 Ω were identical. As a result, the basis of the new proposal was correlated to the value of each single strain gauge output, which would be 0.0734, as shown in Table

Table 4 the comparison between theoretical and simulation outputs

Method	Strain (%)	Vo/Vin (mV/V)	ΔR (Ω)
Theoretical	3.1820E-05	0.114552	0.0401
Simulation	1.1864E-04	0.427104	0.0374

7 Conclusion

The use of information technology in the dynamic system facilitates the management of all processes and ensures the highest degree of precision. Two specialist areas are covered by the strain gauge measurement techniques. These areas are electrical and mechanical engineering. For numerous material tests, the strain that occurs in the material must be identified and measured to facilitate the formulation of essential conclusions about the stability of the structure, regardless of its previous size and shape. The objective of this study is to acquire practical knowledge of resistance strain techniques and to reveal more about the Wheatstone bridge and how it can be applied to strain measurements. The simulation and design of a piezo-resistive metal gauge and torque sensor were reviewed. Equations were derived for the metal gauge found on the torque sensor and torsional shaft. A different material, i.e. aluminum, was selected as the substrate of the strain gauge. The maximum strained locations were identified on the substrate for varying boundary conditions. The gauge pattern was reviewed and designed. The maximum strained area and the corresponding gauge pattern were selected. The simulation results reveal that the strain change of the gauge is linear to the torque applied. The results facilitate the calculation of the percentage of strain transferred from the shaft to the substrate and the gauge. The findings are then used to calculate the individual values of sensor component strain. Instead of building extensive mathematical models by experts, the readily available simulation software has made it possible to model and analyze the operation of a real system by non-experts, who are managers but not programmers.

Acknowledgment

This work was supported by the Mechanical & Materials Engineering Department, Faculty of Engineering & Built Environment of Universiti Kebangsaan Malaysia 43600 UKM Bangi, Malaysia, Department of Mechanical Engineering, College of Engineering, Universiti Tenaga Nasional, Putrajaya Campus, Jalan Ikram-Uniten, 43000 Kajang, Selangor, Malaysia, the Computer Science Department, Faculty of Science, Libyan Sirte University, Sirte, Libya and the Department of Agra-energetics and foods Engineering, Faculty of Mechanical Engineering, Szent Istvan University, H 2103, Godollo, Hungary. They are gratefully acknowledged.

References

Cao, L., Kim, T. S., Mantell, S. C. & Polla, D. L. 2000. Simulation and Fabrication of Piezoresistive Membrane Type Mems Strain Sensors. *Sensors and Actuators A: Physical* 80(3): 273-279.

Eaton, W. P., Bitsie, F., Smith, J. H. & Plummer, D. W. 1999. A New Analytical Solution for Diaphragm Deflection and Its Application to a Surface Micromachined Pressure Sensor. *International Conference on Modeling and Simulation, MSM*, him.

Eberlein, D. 2008. Applying the Wheatstone Bridge Circuit. www.hbm.com [20 September 2015].

Hamid, M. Y., Thangamani, U. & Vaya, P. R. 2006. Simulation of Piezo-Resistive Metal Gauge on Rectangular Membrane for Low-Pressure Application. *Semiconductor Electronics, 2006. ICSE '06. IEEE International Conference on*, him. 304-308.

Hilal Muftah, M. & Haris, S. M. 2011. A Strain Gauge Based System for Measuring Dynamic Loading on a Rotating Shaft. *International Journal of Mechanics* 5(1): 19-26.

Hoffmann, K. 1989. *An Introduction to Measurements Using Strain Gages*. Germany: Hottinger Baldwin Messtechnik GmbH.

Intiang, J., Degollier, E., Rakowski, R. T., Jones, B. E. & Cheshmehdoost, A. 2009 Use of Metallic Resonant Sensor in Torque Measurement Transfer Standard. *SENSOR+TEST Conference 2009 - SENSOR 2009 Proceedings I.*, him.

Joyce, D. & Scott, M. 1993. Force and Mass Determination by Strain Gauge. *Significance of Calibration, IEE Colloquium on*, him. 3/1-310.

Korzenszky, P. 2009. Grinding Kinetic and Energetic Examination of Hammer Mills. Tesis Ph.D., Faculty of Mechanical Engineering, St. István University, Gödöllő, Hungary.

Lin, L., Chu, H.-C. & Lu, Y.-W. 1999. A Simulation Program for the Sensitivity and Linearity of Piezoresistive Pressure Sensors. *Microelectromechanical Systems, Journal of* 8(4): 514-522.

Micro-Measurements, V. 2007. Optimizing Strain Gage Excitation Levels. *Tech Note TN* 502(15.

Muftah, M. & Haris, S. 2010. The Torque Transducer (Sensor) Modify to be Capable of Measuring Dynamical Load During a Rotating Period. *Application of Information and Communication Technologies (AICT), 2010 4th International Conference on*, him. 1-4.

Muftah, M. H., Haris, S. M., Petroczki, K. & Khidir, E. A. 2013. An Improved Strain Gauge-Based Dynamic Torque Measurement Method. *INTERNATIONAL JOURNAL OF CIRCUITS, SYSTEMS AND SIGNAL PROCESSING* 7(1): 66-73.

Murray, W. M. & Miller, W. R. 1992. *The Bonded Electrical Resistance Strain Gage*. Oxford University Press.

Orhan, M. H., Dogan, C., Kocabas, H. & Tepehan, G. 2001. Experimental Strain Analysis of the High-Pressure Strain Gauge Pressure Transducer and Verification by Using a Finite Element Method. *Measurement Science and Technology* 12(3): 335.

Prombonas, A. E., Paralika, M. A. & Poulis, N. A. 2013. Investigation of the Torsional Deformation of the Complete Upper Denture: A Pilot Study.

Schomburg, W., Rummler, Z., Shao, P., Wulff, K. & Xie, L. 2004. The Design of Metal Strain Gauges on Diaphragms. *Journal of Micromechanics and Microengineering* 14(7): 1101.

Szilard, R. 1974. Theory and Analysis of Plates.

Thangamani, U., Mohd Yunus, H. & Ali, C. 2008. Design and Simulation of Force Sensor with Piezo Resistive Rectangular Strain Gauge.

Window, A. L. & Hollister, G. S. 1982. *Strain Gauge Technology*. Applied science publishers.

Yang, M., Ai, C., Wang, N., Sun, X. & Ma, Y. 2008. The Dynamic Torque Measure System Based on Rf Technology. *Control and Decision Conference, 2008. CCDC 2008. Chinese*, him. 1787-1790.

Yang, S. & Lu, N. 2013. Gauge Factor and Stretchability of Silicon-on-Polymer Strain Gauges. *Sensors* 13(7): 8577-8594.

Young, W. C. & Budynas, R. G. 2002. *Roark's Formulas for Stress and Strain*. McGraw-Hill New York.

Zeinali, A., Farzad, A. & Aghkhani, M. 2014. Design, Implementation, and Evaluation of a Torque Transducer with Ability of Real-Time Torque Monitoring. *Journal Of Agricultural Machinery* 4(1): 73-78.

Zorob, A. A. 2010. Building Signal Conditioning for Strain Gauge Sensors. Tesis The Islamic University of Gaza.

Ran Shu, Zhigang Chu and Hongyu Shu, A Lever-Type Method of Strain Exposure for DiskF-Shaped Torque Sensor Design, *1State Key Laboratory of Mechanical Transmissions, Chongqing University, Chongqing 400044, (R.S.); (Z.C.)2College of Automotive Engineering, Chongqing University, Chongqing 400044; Published: 19 January 2020.

Wang Y.J., Zuo G.K., Chen X.L., Liu L. Strain analysis of six-axis force/torque sensors based on analytical method. IEEE Sens.J.2017;17:43944404. http://doi.org/10.1109/JSEN.2017.2703160.

M. Hilal Muftah, K . Petroczki, E. Awad Khidir and A. A. Borhana. Design and Simulation of a Piezoresistive V-Shaped Strain Gauge for Torque Measuring. Scientific Journal for the Faculty of Science-Sirte University Vol 1, No 2, October (2021) 14-51.

Atsuhiro Nishino and Kenichi Fujii. Calibration of a torque measuring device using an electromagnetic force torque standard machine. National Metrology Institute of Japan, AIST, Tsukuba, Ibaraki, Japan. Received 19 September 2018, Revised 27 May 2019, Accepted 14 July 2019, Available online 16 July 2019, Version of Record 30 July 2019.

Misaki Hamaji, Atsuhiro Nishino and Koji Ogushi. Development of a novel dynamic torque generation machine based on the principle of a Kibble balance. Measurement Science and Technology, Volume 33, Number 11 Meas. Sci. Technol. 33 115901 DOI 10.1088/1361-6501/ac8441, 2022.

Cheng Ding; Yong Han; Wei Du; Jianhua Wu State Key Laboratory of Mechanical System, and Vibration, Institute of Robotics, School of Mechanical Engineering, Shanghai Jiao Tong University, Shanghai, China. Published in: IEEE Transactions on Robotics (Volume: 38, Issue: 4, August 2022).

Yu P Manshin, E Yu Manshina, and Mario Geue. About the dynamic error of strain gauge torque measuring devices. Intelligent Information Technology and Mathematical Modeling 2021 (IITMM 2021) Journal of Physics: Conference Series 2131 (2021) 052041 IOP Publishing doi:10.1088/1742-6596/2131/5/052041.